JOURNAL OF SPACECRAFT AND ROCKETS
Vol. 35, No. 1, January–February 1998

Construction Criteria for a Large Space Structure in Low Earth Orbit

Masamichi Shigehara,* Yatsuko Iwasaki,† and Yoko Shigedomi†
Tokyo Metropolitan Institute of Technology, Tokyo 191, Japan
and
Shuichiro Fukuzawa‡
Hokkaido Electric Power Co., Inc., Hokkaido 067, Japan

Such natural environmental torques as the gravity gradient could substantially influence the attitude behavior of a large space structure, especially in a low Earth orbit. Basic criteria are introduced for constructing a large structure in a low-Earth-orbit environment, by using the Solar Power Satellite as a model. The criteria for the basic configuration and construction sequence are derived from the stability map from the rigid-body equations. In addition, two types of multibody equations of motion (chain and octopus) are introduced to examine transient behaviors during construction. Specifically, inertia matrix change, including asymmetrical configuration change, construction speed, internal momentum change, and energy dissipation, are considered. Results from the transient behavior studies are included, in a general level, in a set of construction criteria.

Nomenclature

$\boldsymbol{B}$	= geomagnetic field
$\boldsymbol{D}_i$	= moment of inertia of ith body
$\boldsymbol{f}_i$	= forces on ith body from joint J_i
$\boldsymbol{g}_i$	= sum of gravity gradient and centrifugal forces acting on ith body
$\boldsymbol{H} = [I_x\omega_x \;\; I_y\omega_y \;\; I_z\omega_z]^T$	= angular momentum of the body in roll, pitch, and yaw
$\boldsymbol{I} = [I_x \;\; I_y \;\; I_z]^T$	= inertia matrix of the body
K_i, C_i	= respective spring and damping coefficient of ith joint
$k_x = (I_y - I_z)/I_x$, $k_y = (I_x - I_z)/I_y$, $k_z = (I_y - I_x)/I_z$	= moment of inertia ratio
$\boldsymbol{M}_m$	= dipole moment aboard the body
m_i	= mass of ith body, $M = \sum_{i=1}^{n} m_i$
$\boldsymbol{n}$	= unit vector normal to receiving area, A
$\boldsymbol{n}_i$	= torques on the ith body from joint J_i
$\boldsymbol{q}_i$	= gravity gradient torque around ith body
$\boldsymbol{q}_s(t)$	= gravity gradient torque on overall system, $\boldsymbol{Q}(t) \equiv \boldsymbol{Q}_0 + \int_{t_0}^{t} \boldsymbol{q}_s(t)$
$\boldsymbol{R}$	= distance between center of gravity of the system and center of the Earth
$\boldsymbol{r}_i$	= relative position of ith body to base body ($i = 1$)
$\boldsymbol{r}_i^j$	= relative position of ith joint to base body ($i = 1$)
$\boldsymbol{s}$	= direction of incoming photons
$\boldsymbol{s}_i$	= relative position of ith joint to ith body
$\boldsymbol{T} = [T_x \;\; T_y \;\; T_z]^T$	= applied torque to the body
β_i	= relative angle of ith joint to ith body
η	= orbital angle
ρ_s, ρ_d	= fraction of specular reflection and diffused reflection
(ϕ, θ, ψ)	= Euler angles; attitude of body with respect to reference frame
Ω	= orbital rate
$\boldsymbol{\omega} = [\omega_x \;\; \omega_y \;\; \omega_z]^T$	= angular rate of the body
$\bar{\omega}$	= angular rate of ith body in inertial frame
$[\,]^T$	= transverse matrix

Received March 24, 1997; revision received July 29, 1997; accepted for publication Aug. 1, 1997.

*Professor, Faculty of Aerospace Engineering, 6-6 Asahigaoka, Hino. Member AIAA.
†Graduate Student, Faculty of Aerospace Engineering.
‡Researcher, 2-1 Tsuishikari, Ebetsu.

I. Introduction

DEMANDS for a large space structure that can be constructed simply and easily on orbit in a cost-effective way are increasing. As an example, the future Solar Power Satellite (SPS)[1] will be required to be more reliable and cheaper for it to be a commercially competitive electrical power source for Earth. It would be very helpful if there were construction criteria to meet these demands.

A structure on orbit will have various internal forces/torques, such as the gravity gradient (GG) and centrifugal and fictitious ones caused by the orbital and internal motion within the structure. These force/torques vary highly, depending on the configuration of the structure and its rate of change, creating a complex influence over the motion of the structures during and after construction. In addition, a larger structure tends to receive larger external-disturbance forces/torques such as a solar radiation pressure and air drag.

Extensive analysis has already been done to clarify the attitude behavior of the SPS2000 model, which is a technology demonstration program for future SPS in Japan.[2–5] As shown in Fig. 1, the SPS2000 has a configuration of 300-m length in the north-south (N-S) direction, with a triangular cross section of 300-m height, and will fly in a low Earth equatorial orbit of 1000-km altitude under GG stabilization. One face has a large transmitting antenna, orienting toward the Earth; the other two faces have solar arrays to generate 18 MW of solar power. In constructing the SPS2000, the structural elements are carried up into orbit, module by module, with the final configuration completed after the tenth flight. In the first flight, the base body with triangular cross section and antenna support is assembled on orbit, and then the body is extended along the N-S direction by adding more modules.

In this report, all of these analytical results are used to formulate a set of criteria, in a general level, for constructing a large space structure, especially in low Earth orbit.

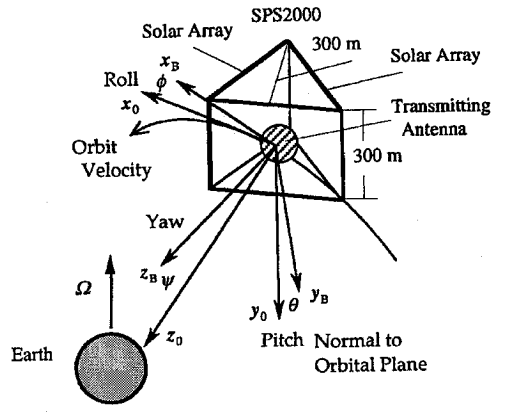

Fig. 1 Configuration of SPS2000 and coordinate frames.

II. Criteria Derived from Static Stability

A. Stability Map Under GG Torque

The fundamental behavior of a large space structure is derived from the equations of motion by assuming a structure as a single rigid body. Let us first define the coordinate systems: The reference coordinate frame $\Phi_0(x_0, y_0, z_0)$ is defined as in Fig. 1, where z_0 is oriented toward the Earth center, x_0 aligning with the orbital velocity, and y_0 normal to the orbital plane. The structure is represented by the body-fixed coordinate frame $\Phi_B(x_B, y_B, z_B)$. The equations of motion of a rigid body are expressed as

$$\left(\frac{d\boldsymbol{H}}{dt}\right)_B + \omega \times \boldsymbol{H} = \boldsymbol{T} \tag{1}$$

where $(d\boldsymbol{H}/dt)_B$ is the angular momentum change observed in the body frame and $\omega \times \boldsymbol{H}$ is a fictitious torque due to the relative rotation of the body frame to the inertial frame. The specific equations and the stability condition can be derived as follows.[6,7] For the body stabilized toward the Earth center, the body rate ω is approximated as

$$\omega = [\omega_x \quad \omega_y \quad \omega_z]_B^T \approx [\dot{\varphi} - \Omega\psi \quad -\Omega + \dot{\theta} \quad \dot{\psi} + \Omega\varphi]^T \tag{2}$$

where the major contributor is the orbital rate. The produced GG torque is approximated for small-attitude offset and near-circular orbit as

$$T_x = -\tfrac{3}{2}\Omega^2(I_y - I_z)\sin 2\varphi \text{ (roll)} \tag{3}$$

$$T_y = -\tfrac{3}{2}\Omega^2(I_x - I_z)\sin 2\theta \text{ (pitch)} \tag{4}$$

Substituting Eqs. (2–4) into Eq. (1), finally we have

$$\ddot{\varphi} + 4\Omega^2 k_x \varphi - \Omega(1 - k_x)\dot{\psi} = 0 \text{ (roll)} \tag{5}$$

$$\ddot{\theta} + 3\Omega^2 k_y \theta = 0 \text{ (pitch)} \tag{6}$$

$$\ddot{\psi} + \Omega^2 k_z \psi + \Omega(1 - k_z)\dot{\varphi} = 0 \text{ (yaw)} \tag{7}$$

Motion in pitch is independent, whereas motion in roll and yaw is coupled through the orbital rate. The moment of inertia ratio (MOIR) determines the stability of the body. The derived stability condition is shown in Fig. 2 as a GG stability map.

The stability map can be used as a tool for checking/deciding the basic configuration and construction sequence of a structure. Here it is applied to the SPS2000, as an example. The SPS2000 will be assembled sequentially, as described in Sec. I. The basic philosophy is first to construct the most stable module on orbit and then gradually to extend toward the N-S direction, i.e., along pitch. This sequence causes a decrease in the GG torque because of increases of MOI in yaw and roll. Still, at the final stage, the MOIR should stay in the stable region. As judged from Fig. 3, the height of the triangle must be equal to or larger than the length of the total beam.

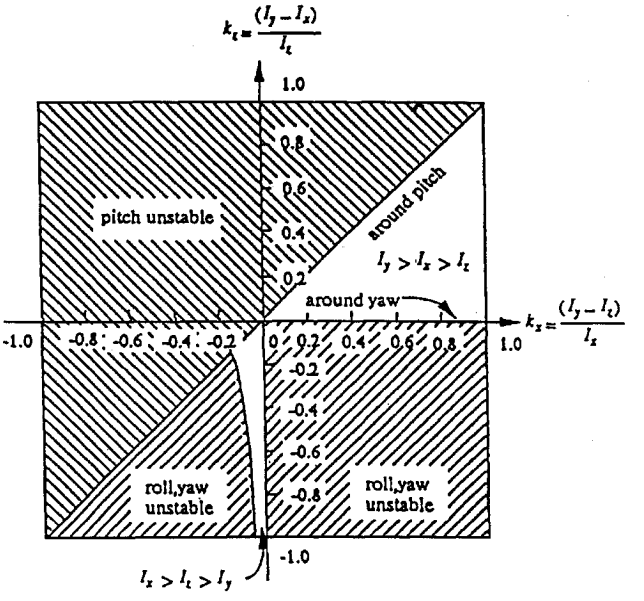

Fig. 2 GG stability map for inertia ratio.

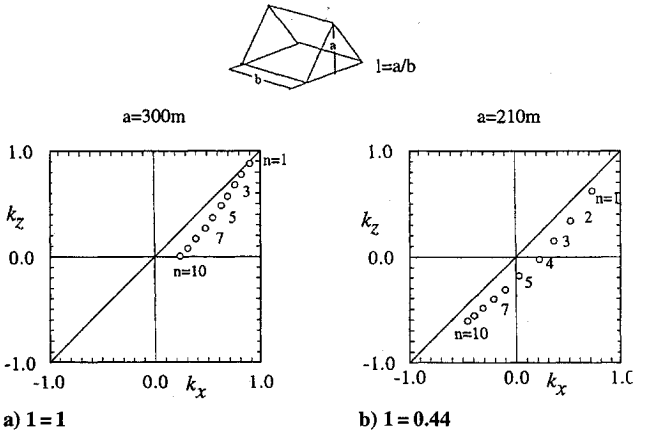

a) 1 = 1 **b) 1 = 0.44**

Fig. 3 Trajectories in stability map for deciding configuration.

For completing the base body, three separate steps, C1, C2, and C3, are required as in Fig. 4. Three sequences of these steps are examined: 1) C1 → C2 → C3, 2) C1 → C3 → C2, and 3) C3 → C1 → C2. In Fig. 5, the travel of the MOIR at every instant of extension is shown for the three sequences. It is found that sequence 3 is desirable because the MOIR stays mostly in the stability region.

B. Restraint on Initial Condition

The initial condition of the body also affects the stability. Although an initial angle offset must be within 90 deg to obtain a stabilizing GG torque, it is expected that, if the body has a large initial rate, the GG restoring torque cannot overcome it before the attitude offset exceeds 90 deg. From Eqs. (6) and (4), we have

$$I_y\ddot{\theta} + q_y \sin 2\theta = 0, \qquad q_y \equiv \tfrac{3}{2}\Omega^2(I_x - I_y) \tag{8}$$

By multiplying $\dot{\theta}$ on both sides of Eq. (8) and integrating, we have

$$\tfrac{1}{2}I_y(\dot{\theta})^2 = E_0 + \tfrac{1}{2}q_y \cos 2\theta \geq 0 \tag{9}$$

where E_0 is an integration constant, representing the total energy of the body. From the condition that the right-hand side of Eq. (9) cannot be negative, 1) if $q_y/2E_0 \leq 1$, θ can be any angle; and 2) if $q_y/2E_0 > 1$, θ must be $-\theta_{\text{lim}} < \theta < \theta_{\text{lim}}$. Thus, condition 2 must be met to be stable:

$$q_y > 2E_0 = I_y\dot{\theta}_0^2 - q_y; \qquad \text{thus} \qquad q_y > \tfrac{1}{2}I_y\dot{\theta}_0^2 \tag{10}$$

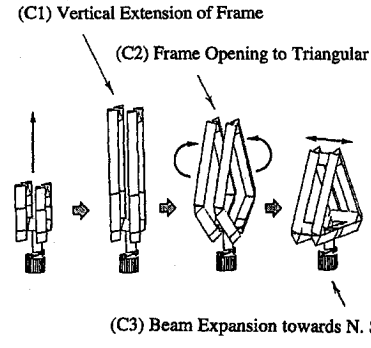

Fig. 4 Expansion sequence of basic module.

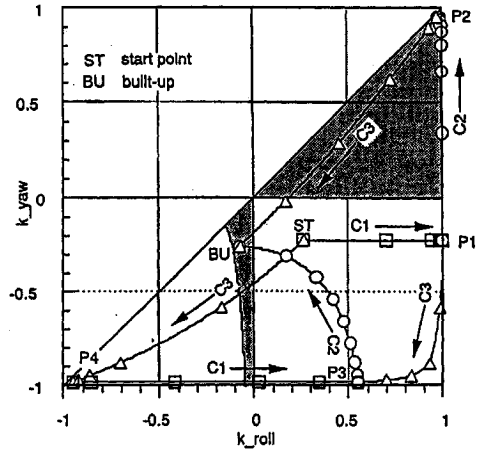

Fig. 5 Trajectories in GG map for three typical expansion sequences: □, (C1) vertical extension of frame; ○, (C2) frame opening to triangular shape; and △, (C3) beam extension toward N-S.

For roll and yaw motions, the same logic is applicable if the cross coupling between roll and yaw is negligible. Thus, for maintaining the stability, the initial rate around each axis must satisfy

$$\dot{\theta}_0 < \Omega\sqrt{3(I_x - I_z)/I_y} = \Omega\sqrt{3k_y} \text{ (pitch)} \qquad (11)$$

$$\dot{\varphi}_0 < \Omega\sqrt{4k_x} \text{ (roll)}, \qquad \dot{\psi}_0 < \Omega\sqrt{k_z} \text{ (yaw)} \qquad (12)$$

III. Criteria Derived from Dynamic Stability

In a practical assembly and construction, there can be such cases as 1) appendages that are extending from the base body, 2) assembling robots that are transporting the secondary structure along the base body, 3) robot arm that is slewing, 4) an additional structure that is attached to the base body, and 5) a joint between the structures that has a compliance such as a spring constraint or energy dissipation, e.g., friction.

From the physical standpoint, these cases can be categorized as motion under the following conditions.

1) Change of inertia matrix

a) Magnitude change of moment of inertia,

b) Change of inertia matrix creating cross product: asymmetrical configuration;

2) Internal change of angular momentum;

3) Reaction due to internal force/torque, including energy dissipation.

A single rigid-body model can no longer handle these factors, and so two types of multibody models are introduced: One is the multichain-body model, where the bodies are connected serially, like a chain (Fig. 6); the other is the so-called octopus-type multibody model,[5] where the bodies are connected radially from the base body (Fig. 7).

A. Multichain Body with Flexible Joints

First, a multichain-body model is studied, where the nth body is connected to the $(n-1)$th body through a joint. The joint has a single

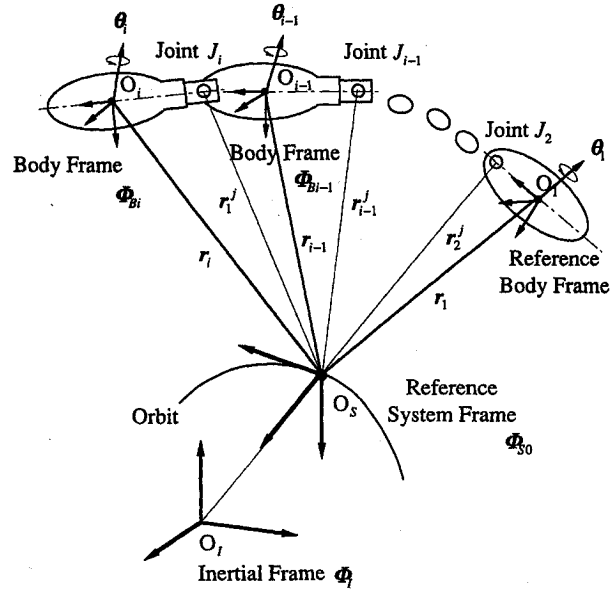

Fig. 6 Multichain-body model with flexible joints.

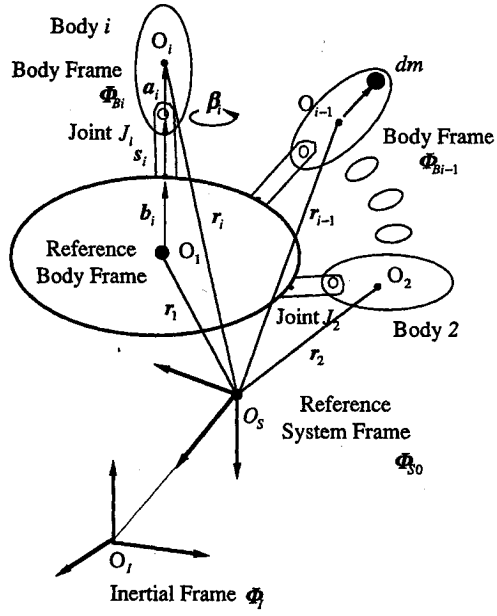

Fig. 7 Multibody model (octopus type).

degree of freedom for translation along the body axis to which it connects and three degrees of freedom for rotation. The joint has a compliance represented by the spring and damping torques.

Different from motions on the ground, base-body 1 is not fixed but moves in orbit under the force of gravity.[8] Thus the equations of motion must be written both for base-body 1 [or center of gravity (CG) of the total system] and for the relative motion of the nth body with respect to base-body 1. The equations of motion can be derived through formulating the Lagrange equations for the overall system.

The derived equations are expressed as follows.

1) Translational motion of the CG of the overall system,

$$M\frac{d^2\boldsymbol{R}}{dt^2} + M\frac{\mu}{R^3}\boldsymbol{R} \approx 0 \qquad (13)$$

2) Rotational motion of the overall system around the CG,

$$\sum_{i=1}^{n} m_i \frac{d}{dt}\left(\boldsymbol{r}_i \times \frac{d\boldsymbol{r}_i}{dt}\right) + \sum_{i=1}^{n} \frac{d}{dt}(\boldsymbol{D}_i\bar{\omega}_i) = \boldsymbol{q}_s(t) \qquad (14)$$

$$\bar{\omega}_i \equiv \sum_{m=2}^{i} \dot{\beta}_m + \bar{\omega}_1$$

3) Translational motion of the ith body,

$$m_i \frac{\mathrm{d}^2 \boldsymbol{r}_i}{\mathrm{d}t^2} = \boldsymbol{g}_i + \boldsymbol{f}_i - \boldsymbol{f}_{i+1} \qquad (i = 1 \text{ to } n) \tag{15}$$

4) Rotational motion of the ith body,

$$\frac{\mathrm{d}}{\mathrm{d}t}(\boldsymbol{D}_i \bar{\omega}_i) = \boldsymbol{q}_i + \boldsymbol{n}_i - \boldsymbol{n}_{i+1} + \left(\boldsymbol{r}_i^j - \boldsymbol{r}_i\right) \times \boldsymbol{f}_i - \left(\boldsymbol{r}_{i+1}^j - \boldsymbol{r}_i\right) \times \boldsymbol{f}_{i+1} + \left(-K_i \beta_i + K_{i+1}\beta_{i+1} - C_i \dot{\beta}_i + C_{i+1}\dot{\beta}_{i+1}\right) \qquad (i = 1 \text{ to } n) \tag{16}$$

5) Equation of the CG point,

$$\sum_{i=1}^{n} m_i \boldsymbol{r}_i = 0 \qquad \text{or} \qquad \sum_{i=1}^{n} m_i \frac{\mathrm{d}^2 \boldsymbol{r}_i}{\mathrm{d}t^2} = 0 \tag{17}$$

Equations (13–17) are the fundamental ones for the multichain-body systems but, in a practical analysis, they must be tailored to the relative coordinate systems. In Secs. III.B–III.E, the results are shown by applying these equations to the representative dynamic categories.

First, let us examine the kinematic model, where the position, angle, and rate of the ith body are given with time, such as for a beam extension with a constant speed or for a preprogrammed work by the robot. For these cases, the dynamic equations (15) and (16) for the ith body become unnecessary. The translational motion of base-body 1 can be obtained from Eq. (17), representing the conservation of total momentum, as

$$M\dot{\boldsymbol{r}}_1 + \sum_{i=2}^{n}\left[\left(\sum_{m=i}^{n} m_m\right)\dot{\boldsymbol{s}}_i\right] + \sum_{i=2}^{n}\dot{\beta}_i \times \left[\sum_{m=i}^{n} m_m\left(\boldsymbol{r}_m - \boldsymbol{r}_i^j\right)\right] = 0 \tag{18}$$

where the second and third terms on the left-hand side of Eq. (18) are the respective momentum changes caused by movement of joint J_i and rotation of joint J_i. The rotation of base-body 1 is defined from Eq. (14) as

$$\left(\sum_{i=1}^{n}\boldsymbol{D}_i\right)\bar{\omega}_1 + \sum_{i=1}^{n}[\boldsymbol{r}_i \times (\bar{\omega}_1 \times m_i \boldsymbol{r}_i)] + \sum_{i=2}^{n}\left[\left(\sum_{m=i}^{n} m_m \boldsymbol{r}_m\right) \times \dot{\boldsymbol{s}}_i\right] + \sum_{i=2}^{n}\left(\sum_{m=i}^{n}\boldsymbol{D}_m\right)\dot{\beta}_i + \sum_{i=2}^{n}\left\{\sum_{m=i}^{n}\boldsymbol{r}_m \times \left[\dot{\beta}_i \times m_m\left(\boldsymbol{r}_m - \boldsymbol{r}_i^j\right)\right]\right\} = \boldsymbol{Q}(t) \tag{19}$$

where the second, third, and fourth terms on the left-hand side of Eq. (19) are the respective angular momentum change around the CG of the system caused by rotation of base-body 1, translation of joint J_i, and rotation of joint J_i; the fifth term is relative momentum change caused by rotation of joint J_i.

B. Motion by Magnitude Change of MOI

The typical model, corresponding to the preceding equations, is given as in Fig. 8a, where a truss extends along the local vertical. Assuming the two-body system $n = 2$ and $\dot{\beta}_i = 0$, we have from Eq. (18)

$$(m_1 + m_2)\dot{\boldsymbol{r}}_1 + m_2\dot{\boldsymbol{s}}_2 = 0; \quad \text{thus} \quad \dot{\boldsymbol{r}}_1 = -\frac{m_2}{(m_1 + m_2)}\dot{\boldsymbol{s}}_2 \tag{20}$$

After the end of the extension, $\dot{\boldsymbol{r}} = 0$. From Eq. (19), under $\dot{\beta}_i = 0$,

$$\left(\sum_{i=1}^{2}\boldsymbol{D}_i\right)\bar{\omega}_1 + \sum_{i=1}^{2}[\boldsymbol{r}_i \times (\bar{\omega}_1 \times m_i \boldsymbol{r}_i)] + \sum_{i=2}^{2}\left[\left(\sum_{m=i}^{2} m_m \boldsymbol{r}_m \times \dot{\boldsymbol{s}}_i\right)\right] = \boldsymbol{Q}(t) \tag{21}$$

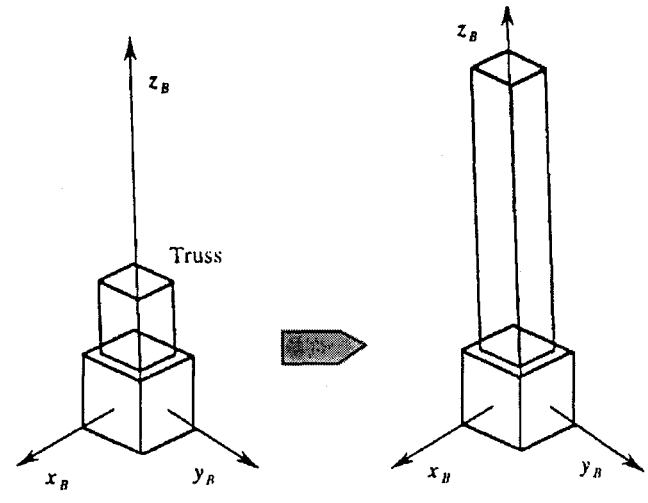

Fig. 8 Attitude and MOI histories under truss extension along local vertical: □, roll; ○, pitch; and △, yaw.

Because $\boldsymbol{r}_m$ and $\dot{\boldsymbol{s}}_m$ are in the same direction, the third term of Eq. (21) is zero. Equation (21) becomes, under $\boldsymbol{r}_1 = 0$,

$$\sum_{i=1}^{n}\boldsymbol{D}_i \equiv I_0, \qquad I_2 \equiv m_2 r_2^2$$

$$I_0\bar{\omega}_1 + \boldsymbol{r}_2 \times (\bar{\omega}_1 \times m_2\boldsymbol{r}_2) = (I_0 + I_2)\bar{\omega}_1 = \boldsymbol{Q} \tag{22}$$

where I_2 corresponds to an increase of the MOI due to extension. The body orienting toward the local vertical initially has an angular momentum $I_0\Omega = Q_0$ in pitch, given by orbital rate Ω, and this angular momentum is conserved if the GG torque is neglected during extension. Thus, from Eq. (22),

$$(I_0 + I_2)\bar{\omega}_1(t) = I_0\Omega; \quad \text{then} \quad \bar{\omega}_1(t) = \frac{I_0}{(I_0 + I_2)}\Omega \tag{23}$$

This indicates that the body rate reduces when the MOI increases. As in Fig. 8b, the MOI in pitch and roll increases by about 15 times, in 100 min, at the end of the extension. Thus, as shown in Fig. 8c, the attitude of the base body deviates backward from the local vertical and then the GG torque restores the deviation as the angle of deviation increases. A case study for a decrease of MOI also is performed: As the MOI in pitch decreases, the angular rate of the body increases, resulting in a transient attitude drift forward from the local vertical.

In summary, at all times, change of configuration around pitch must be designed carefully because any MOI change in pitch will change the base-body rate in pitch, causing an attitude deviation from the local vertical.

C. Change of Inertia Matrix Creating Cross Product, Asymmetrical Configuration

The effect of change of inertia matrix, such as by configuration change during construction, also is studied. The effect of asymmetrical configuration vs symmetrical one can be analyzed by using the octopus-type multibody model, as defined in Fig. 7. The equations of motion can be derived by applying the same principle as for the multichain model. The simplified kinematic model is assumed to be as in Fig. 9, representing construction masses (secondary bodies) that are transferred along the base structure in various routes, such as from B to C or B to E via C. The model also can simulate a change by moving the plural bodies in a symmetrical fashion, such as one from B to C and the other from B to Cc.

Figures 10–12 show the typical results for asymmetrical configuration change by moving a single body from B to C. Because of this move, the cross product of inertia matrix change around pitch and yaw is created as shown in Fig. 10. This offsets the principal axes of the base body from the original axes. Thus, at the end of the move, the base body will oscillate around these new principal axes, as in Fig. 11, where the offset of the center of oscillation is equal to the offset of the principal axes.

The effect of the construction speed also is examined by varying the speed of the moving body in the same model. The resultant amplitude of oscillation is shown in Fig. 12 relative to time to end of the move (reciprocal to speed). Because similar results are obtained

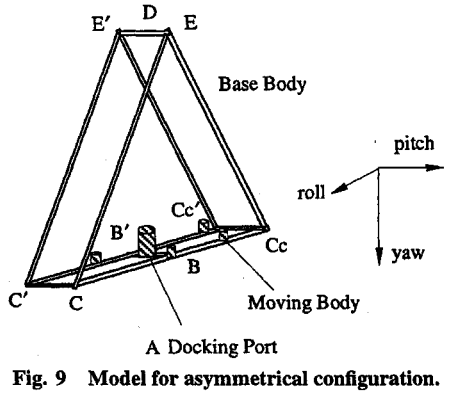

Fig. 9 Model for asymmetrical configuration.

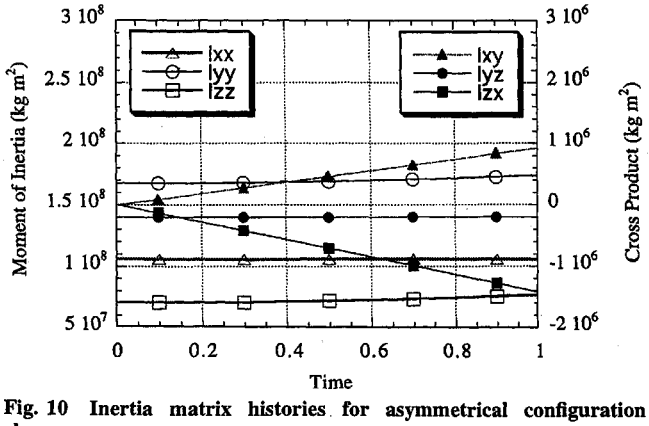

Fig. 10 Inertia matrix histories for asymmetrical configuration change.

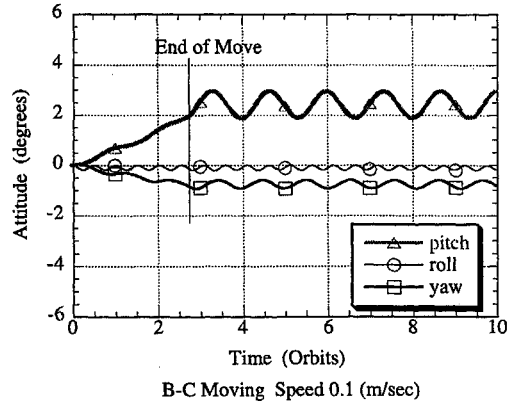

Fig. 11 Attitude histories for asymmetrical configuration change.

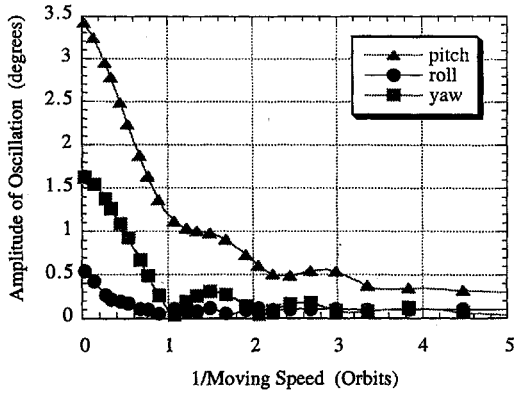

Fig. 12 Resultant amplitude of oscillation vs moving speed.

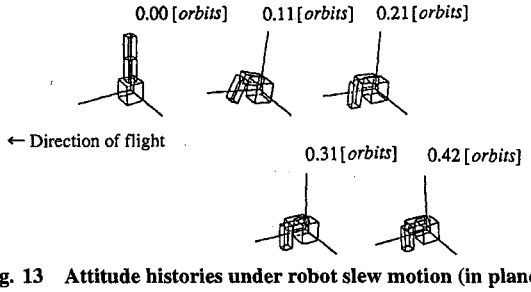

Fig. 13 Attitude histories under robot slew motion (in plane).

for all of the other simulation cases, it can be said that the resultant amplitude of deviation will decrease drastically by decreasing the speed of the move. This is mainly because the slower the move, the longer the transient time, which allows the GG torque to restore the deviation caused by the momentum of the moving body.

Thus, it is concluded that the configuration and its change should be as symmetrical as possible during construction because the asymmetrical configuration will shift the attitude reference (principal axes) of the body. Also, the construction speed should be kept within a certain limit to avoid excessive attitude deviation, especially when the MOI is decreasing, because a decrease of MOI reduces the GG restoring torque.

D. Motion by Internal Change of Angular Momentum

The effect of rotational motion of the internal structures also can be analyzed by the multichain kinematic model. As shown in Fig. 13 as an example, the two robot arms are slewing by 90 deg with a speed of 0.1 deg/s in pitch. During slew, the motion of the arms causes the base body to move in the opposite direction, in the same manner as a command torque to a momentum wheel imparts an equal and opposite reactive torque to the spacecraft. However, after the end of the slew, this motion will stop, and the GG torque tends to reduce the deviation to zero.

Any internal movement of the structural elements creates an attitude deviation of a base body through the momentum exchange. This deviation is dependent on the speed, the applied time duration, and the ratio of the MOI of the moving elements to the base body.

E. Effect of Damping Mechanisms and Flexibility of Structure

If the construction is done in such a way that internal force/torque is applied to the joints, Eqs. (17) and (14) must be solved, combined with Eqs. (15) and (16), as a dynamic model. As a typical example, the effect of the damper is studied by assigning the damping torque to the joints. Typical results under the damping torque of 1.0 N · m · s/rad are shown in Fig. 14, as compared with the results without the damper, where the two secondary appendages extend vertically with a given acceleration speed.

The effect of the damper on the oscillation is significant, and thus a structure must have some sort of damping devices[9] installed because, by its nature, the GG torque produces an oscillation. In this paper, for clarity, no damper is assumed in all other simulations, but all oscillations that appear in the figures will be damped out if a proper damper is installed.

The extent of the effect of flexibility of a structure could be evaluated by assuming the two extreme cases: model of rigid joints and model of free joints. The specific analysis can be done by giving the equivalent compliance, e.g., spring and damping coefficient, to the joints.

IV. Disturbance Torque and Its Compensation

A. Disturbance Torque

Disturbance torque is another factor in deciding the configuration and construction methodology. In Table 1, the representative disturbance torque level acting on a structure in a low Earth orbit is given relative to the GG torque. Solar radiation has significant influence if a structure having a larger solar array area is being considered.

A solar radiation pressure of $P = 4.5 \times 10^{-6}$ N/m^2, acting on the area of A m^2, will create the force $\boldsymbol{F}_s$ given by[10]

$$\boldsymbol{F}_s = PA(\boldsymbol{n}\cdot\boldsymbol{s})\{(1-\rho_s)\boldsymbol{s} + 2[\rho_s(\boldsymbol{n}\cdot\boldsymbol{s}) + \tfrac{1}{3}\rho_d]\boldsymbol{n}\} \tag{24}$$

Table 1 Level of disturbance torque

Source of torque	Equation	Typical torque level, N-m
Gravity gradient	$3\Omega^2(I_x - I_z)\theta$	3×10^{-2}
Solar radiation	$\Delta y \cdot PA$	4.5×10^{-1}
Magnetic	$M \cdot B$	1

If there is an offset $\boldsymbol{r}_s$ between this center of pressure (CP) and the CG, the torque $\boldsymbol{T}_s = \boldsymbol{r}_s \times \boldsymbol{F}_s$ will be produced. If the SPS2000 model is assumed, the offset $\boldsymbol{r}_s$ can be close to zero in roll/yaw because of symmetry of its configuration, whereas, in pitch certain levels of $\boldsymbol{r}_s$ are produced, depending on the orbital position. The calculation result for the SPS2000, as shown in Fig. 15, indicates that the solar radiation torque has a fundamentally sinusoidal variation with an orbital period.

If this torque is expressed in a simpler form as $T_s = T_0 \sin \Omega t$, then the equation of motion in pitch of the system, from Eq. (6), becomes

$$I_y\ddot{\theta} + 3I_y\Omega^2 k_y\theta = T_s \sin \Omega t \tag{25}$$

Under a forced oscillatory torque of frequency Ω, the system will oscillate, having the same frequency Ω with phase delay α as

$$\theta = \frac{(T_0/I_y)}{\Omega^2(3k_y - 1)} \sin(\Omega t - \alpha) \tag{26}$$

Because the value of $(3k_y)^{1/2}$ is close to 1 in a normal case, the system will oscillate in a nearly resonant mode, causing a large attitude deviation. Thus, this solar pressure torque should be eliminated by applying an appropriate control scheme.

B. Geomagnetic Control Torque

Among the various control schemes, the use of geomagnetic torque is most suitable for a large space structure because of its simplicity and long life. The dipole moment aboard the body will produce a torque in a geomagnetic field as $\boldsymbol{T} = \boldsymbol{M}_m \times \boldsymbol{B}$. If the polarity and amplitude of $\boldsymbol{M}_m$ are chosen by using an appropriate algorithm depending on $\boldsymbol{B}$, the desired control torque will be produced.[4,11]

The geomagnetic pole declines by $\delta = 11.4$ deg to the geographical pole of the Earth, and the component of $\boldsymbol{B}$ is expressed approximately in an equatorial orbit as

$$\boldsymbol{B} = \begin{bmatrix} B\sin\delta\sin\eta \\ -B\cos\delta \\ B\sin\delta\cos\eta \end{bmatrix} \tag{27}$$

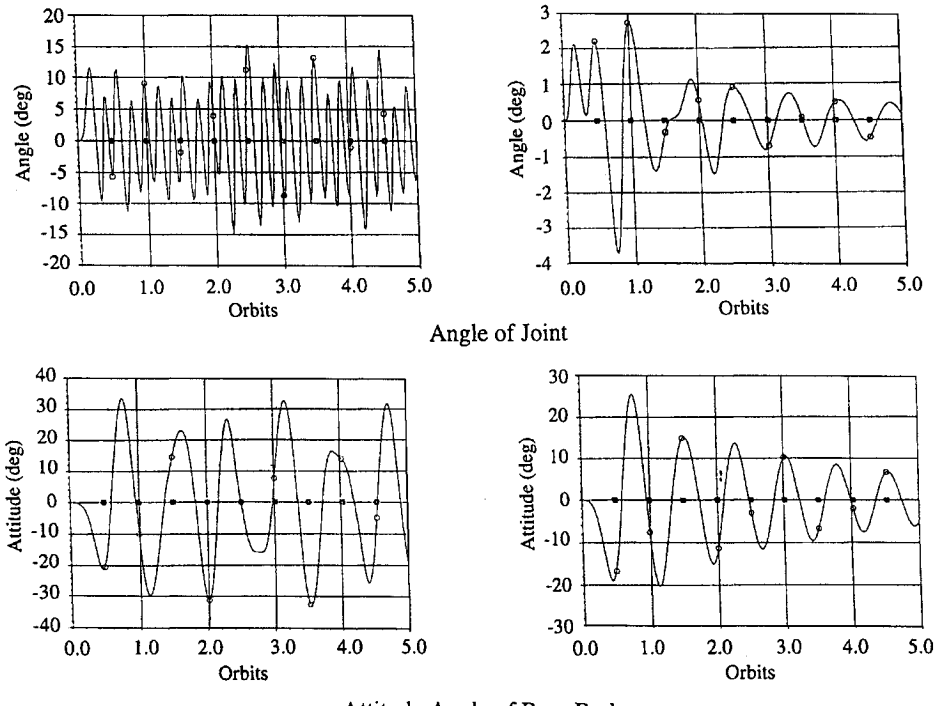

a) Without damper **b) With damper**

Fig. 14 Effect of damper on oscillation.

Table 2 Summary of criteria for construction

Cause	Example	Effect	Criteria
Mass distribution	Configuration during/after construction	To produce dependent GG torque	MOIR should stay in the stable region
Initial condition	Initial attitude offset Initial rate	To produce dependent GG torque Increase/decrease of angle offset	Offset should be within 90 deg Initial rate should be within the limit
Magnitude change of MOI ΔI	Truss extension Frame opening Mass transportation	To create body rate change in pitch $\Delta I > 0$: backward body rate $\Delta I < 0$: forward body rate	Change of speed should be controlled so that GG can be restored before attitude exceeds 90 deg Careful attention when $\Delta I < 0$
Product of inertia	Asymmetrical Extension, construction	To change principal axes, causing motion to shift around new principal axis	Shifted motion must be within the limit Symmetrical configuration is desirable
Speed of MOI change	Mass transportation	Higher speed creates larger attitude deviation	Speed must be controlled within a limit
Local change of angular momentum	Array extension Robot slew motion	To rotate the body in opposite direction to conserve total momentum	Change must be comparatively small
Energy dissipation	Damper Compliance of joints	To damp out vibration	Structure should have some sort of energy dissipator
Disturbance torque	Solar radiation Geomagnetic Air drag	To increase or decrease attitude rate	Control torque must be applied when disturbance exceeds GG

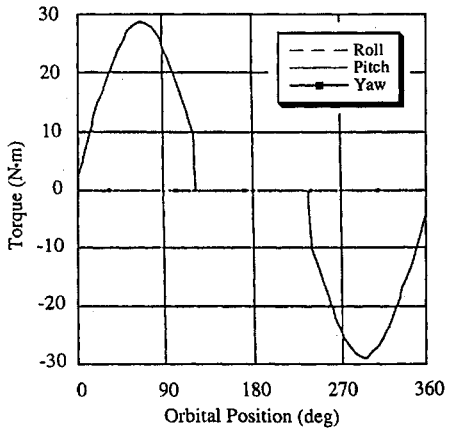

Fig. 15 Solar radiation torque.

If the control dipole is assumed as $\boldsymbol{M}_m = [M_x \;\; 0 \;\; M_z]^T$ to reduce the undesirable torque in roll and yaw, then

$$\boldsymbol{T} = \boldsymbol{M}_m \times \boldsymbol{B} = \begin{bmatrix} M_x \\ 0 \\ M_z \end{bmatrix} \times \begin{bmatrix} B_x \\ B_y \\ B_z \end{bmatrix}$$

$$= B \begin{bmatrix} M_z \cos\delta \\ M_z \sin\delta \sin\eta - M_x \sin\delta \cos\eta \\ -M_x \cos\delta \end{bmatrix} \tag{28}$$

Further, if $M_x = 0$ is assumed to minimize the torque in yaw, the torque produced becomes

$$\boldsymbol{T} = \boldsymbol{M}_m \times \boldsymbol{B} = BM_z \begin{bmatrix} \cos\delta \\ \sin\delta \sin\eta \\ 0 \end{bmatrix} \tag{29}$$

If the control torque is applied at around $\eta = \pi/2 \pm n\pi$ (n = integer), then the control torque in pitch can be maximized while keeping the disturbance torque in roll constant.

The simulation results show the practical applicability of the geomagnetic control to compensate for the solar radiation torque, even in pitch.

V. Summary and Conclusions

Natural environmental torques such as the GG and geomagnetic and solar radiation pressure torque substantially influence the attitude behavior of a large space structure, depending on its configuration and its rate of change. These behaviors have been analyzed by use of both a single rigid body and a multibody model, and the results obtained have been integrated and summarized in Table 2 to provide the construction criteria at a general level.

Acknowledgments

Part of this study was conducted under a special research fund from the Tokyo Metropolitan Institute of Technology. Thanks are due to the colleagues of the SPS2000 working group.

References

[1]Nagatomo, M., "10MW Satellite Power System: A Space Station Mission Beyond 2000," *Space Power*, Vol. 6, No. 2, 1986, pp. 299–304.

[2]Shigehara, M., and Ohtaka, A., "A Construction Methodology of the Large Solar Array System of a Solar Power Satellite," *Acta Astronautica*, Vol. 38, Nos. 4–8, 1996, pp. 223–229.

[3]Fukuzawa, S., Modi, V. J., and Nagatomo, M., "On the Construction Methodology and Dynamical Formulation for the Proposed Solar Power Satellites SPS2000," *19th International Symposium on Space Technology and Science (ISTS)* (Yokohama, Japan), ISTS 94-e-06, 1994, pp. 1–4.

[4]Shigehara, M., and Fukuzawa, S., "A Construction Methodology of the Large Space Structures Under Gravity Gradient Stabilization," *3rd Pacific International Congress of Aero and Space Technology (PICAST)* (Melbourne, Australia), 1995, pp. 1–7.

[5]Shigehara, M., and Shigedomi, Y., "A Multibody Model Approach to Obtain the Construction Criteria for a Large Space Structure," *48th International Astronautical Congress* (Turin, Italy), IAF-97-A-1.0.8, 1997, pp. 1–8.

[6]Kaplan, M. H., *Modern Spacecraft Dynamics and Control*, Wiley, New York, 1976, pp. 199–204.

[7]Wertz, R. J., *Spacecraft Attitude Determination and Control*, Kluwer Academic, Boston, 1978, pp. 608–612.

[8]Malla, R. B., "Motion and Deformation of Very Large Space Structures," *AIAA Journal*, Vol. 27, No. 3, 1989, pp. 374–376.

[9]Arduini, C., and Baiocco, P., "Active Magnetic Damping Attitude Control for Gravity Gradient Stabilized Spacecraft," *Journal of Guidance, Control, and Dynamics*, Vol. 20, No. 1, 1997, pp. 117–122.

[10]Chobotov, V. A., *Spacecraft Attitude Dynamics and Control*, Krieger, Malabar, FL, 1991, pp. 77–80.

[11]Shigehara, M., "Geomagnetic Attitude Control of an Axisymmetric Spinning Satellite," *Journal of Spacecraft and Rockets*, Vol. 9, No. 6, 1972, pp. 391–398.

R. B. Malla
Associate Editor